BMC
Cancer

RESEARCH ARTICLE   **Open Access**

Feasibility of a multimodal ^{18}F-FDG-directed lymph node surgical excisional biopsy approach for appropriate diagnostic tissue sampling in patients with suspected lymphoma

Stephen P Povoski[1*], Nathan C Hall[2,3], Douglas A Murrey Jr[2], Chadwick L Wright[2] and Edward W Martin Jr[1]

Abstract

Background: ^{18}F-FDG PET/CT imaging is widely utilized in the clinical evaluation of patients with suspected or documented lymphoma. The aim was to describe our cumulative experience with a multimodal ^{18}F-FDG-directed lymph node surgical excisional biopsy approach in patients with suspected lymphoma.

Methods: Thirteen patients (mean age 51 (±16;22–76) years), with suspected new or suspected recurrent lymphoma suggested by ^{18}F-FDG-avid lesions seen on prior diagnostic whole-body PET/CT imaging, were injected IV with ^{18}F-FDG prior to undergoing same-day diagnostic lymph node surgical excisional biopsy in the operating room. Various ^{18}F-FDG detection strategies were used on the day of surgery, including, (1) same-day pre-resection patient PET/CT; (2) intraoperative gamma probe assessment; (3) clinical scanner specimen PET/CT imaging of whole surgically excised tissue specimens; (4) specimen gamma well counts; and/or (5) same-day post-resection patient PET/CT.

Results: Same-day ^{18}F-FDG injection dose was 14.8 (±2.4;12.5-20.6) millicuries or 548 (±89;463–762) megabecquerels. Sites of ^{18}F-FDG-avid lesions were 4 inguinal, 3 cervical, 3 abdominal/retroperitoneal, 2 axillary, and 1 gluteal region subcutaneous tissue. Same-day pre-resection patient PET/CT was performed on 6 patients. Intraoperative gamma probe assessment was performed on 13 patients. Clinical scanner PET/CT imaging of whole surgically excised tissue specimens was performed in 10 cases. Specimen gamma well counts were performed in 6 cases. Same-day post-resection patient PET/CT imaging was performed on 8 patients. Time from ^{18}F-FDG injection to same-day pre-resection patient PET/CT, intraoperative gamma probe assessment, and same-day post-resection patient PET/CT were 76 (±8;64–84), 240 (±63;168–304), and 487 (±104;331–599) minutes, respectively. Time from ^{18}F-FDG injection to clinical scanner PET/CT of whole surgically excised tissue specimens was 363 (±60;272–446) minutes. Time from ^{18}F-FDG injection to specimen gamma well counts was 591 (±96;420–689) minutes. Intraoperative gamma probe assessment successfully identified ^{18}F-FDG-avid lesions in 12/13 patients. Histopathologic evaluation confirmed lymphoma in 12/13 patients and benign disease in 1/13 patients.

Conclusions: A multimodal approach to ^{18}F-FDG-directed lymph node surgical excisional biopsy for suspected lymphoma is technically feasible for guiding appropriate diagnostic tissue sampling of lymph nodes seen as ^{18}F-FDG-avid lesions on diagnostic ^{18}F-FDG PET/CT imaging.

Keywords: ^{18}F-FDG, PET/CT, ^{18}F-FDG-directed surgery, Real-time, Oncologic, Lymphoma

* Correspondence: stephen.povoski@osumc.edu
[1]Division of Surgical Oncology, Department of Surgery, Arthur G. James Cancer Hospital and Richard J. Solove Research Institute and Comprehensive Cancer Center, The Ohio State University Wexner Medical Center, Columbus, OH 43210, USA
Full list of author information is available at the end of the article

BioMed Central

Povoski *et al. BMC Cancer* (2015) 15:378

Page 2 of 8

Background

Diagnostic ^{18}F-fluorodeoxyglucose (^{18}F-FDG) positron emission tomography/computed tomography (PET/CT) imaging is widely utilized in the clinical assessment of patients with lymphoma, including for initial staging, treatment monitoring during therapy, restaging after completion of therapy, and detection of suspected recurrent disease [1-13]. These various applications of diagnostic ^{18}F-FDG PET/CT imaging can dramatically influence management/therapy recommendations for lymphoma patients and can have the potential to positively impact upon long-term patient outcomes.

The surgeon has continued to play an important role in facilitating the diagnostic pathway for patients with suspected new or suspected recurrent lymphoma, as the findings noted on diagnostic ^{18}F-FDG PET/CT imaging that are considered suspicious for lymphoma frequently require the subsequent performance of a lymph node surgical excisional biopsy procedure for confirmation of a definitive diagnosis [14], as well as for histopathologic, immunophenotypic, flow cytometry, and molecular subtype analyses [15].

Over the last 15 years, there has been increasing interest by surgeons and nuclear medicine/molecular imaging physicians in utilizing ^{18}F-FDG and PET/CT imaging technology to attempt to provide real-time information within the operative room and perioperative setting for cancer patients [16-75]. Specifically related to our collaborative efforts at The Ohio State University, we have previously investigated the use of a novel, multimodal imaging and detection approach involving perioperative patient and *ex vivo* surgical specimen ^{18}F-FDG PET/CT imaging in combination with intraoperative ^{18}F-FDG gamma probe detection [61]. In this regard, the aim of this study was to describe our cumulative experience in patients with suspected new or suspected recurrent lymphoma with a multimodal approach to ^{18}F-FDG-directed lymph node surgical excisional biopsy for guiding appropriate diagnostic tissue sampling of lymph nodes that are seen as ^{18}F-FDG-avid lesions on prior diagnostic whole-body ^{18}F-FDG PET/CT imaging.

Methods

All aspects of the current retrospective analysis were approved by the Cancer Institutional Review Board (IRB) at The Ohio State University Wexner Medical Center. The data for the current retrospective analysis were acquired from a master prospectively-maintained database (with database inclusion dates from June 2005 to June 2012), which were generated from the combination of several Cancer IRB-approved protocols, and which involved a multimodal imaging and detection approach to ^{18}F-FDG-directed surgery for the localization and resection of ^{18}F-FDG-avid lesions in patients with known and

suspected malignancies. This multimodal imaging and detection approach to ^{18}F-FDG-directed surgery included 166 patients who gave consent to participate in one of the IRB-approved protocols, and a total of 157 patients who eventually were taken to the operating room for ^{18}F-FDG-directed surgery.

The imaging parameters of this multimodal imaging and detection approach to ^{18}F-FDG-directed surgery have been previously described in significant detail elsewhere [61,74]. All participating patients received a same-day single-dose preoperative intravenous injection of ^{18}F-FDG. All patients fasted for a minimum of 6 hours prior to receiving their same-day single-dose preoperative intravenous injection of ^{18}F-FDG. Various ^{18}F-FDG detection strategies were used, including: (1) same-day pre-resection whole body or limited field of view patient PET/CT scan (consisting of 6 to 8 field of view PET bed positions for whole body imaging with 2 minutes of PET imaging per each PET bed position or consisting of 1 to 3 field of view PET bed positions for limited field of view imaging with 2 minutes of PET imaging per each PET bed position); (2) intraoperative gamma probe assessment; (3) clinical scanner PET/CT imaging of whole surgically excised tissue specimens (consisting of 1 field of view PET bed position for 10 minutes); (4) specimen gamma well counting; and/or (5) same-day post-resection limited field of view patient PET/CT scan (consisting of 1 to 3 field of view PET bed positions, with 10 minutes of PET imaging per each PET bed position). The ^{18}F-FDG PET/CT images were acquired on one of three clinical diagnostic scanners: (1) Siemens Biograph 16 (Siemens, Knoxville, Tennessee); (2) Phillips Gemini TF (Philips, Amsterdam, Netherlands); and (3) Siemens Biograph 64 Slice mCT (Siemens, Knoxville, Tennessee). The ^{18}F-FDG PET/CT images were all analyzed on a Philips Extended Brilliance Work Station (Philips, Amsterdam, Netherlands). For each individual patient, the same-day preoperative diagnostic ^{18}F-FDG PET/CT scan, the same-day postoperative diagnostic ^{18}F-FDG PET/CT scan, and the whole surgically excised tissue specimen PET/CT scan were performed on the same clinical diagnostic scanner.

All presumed ^{18}F-FDG-avid lesions seen on diagnostic ^{18}F-FDG PET/CT imaging were reported out with a maximum standard uptake value (SUVmax) on each presumed ^{18}F-FDG-avid lesion. Likewise, there was no "minimal set threshold value" for the SUVmax on any given presumed ^{18}F-FDG-avid lesion to be considered as a designation of an "abnormal" hypermetabolic ^{18}F-FDG-avid focus and to be reported out as "suspicious for malignancy". Rather, the determination of any given presumed ^{18}F-FDG-avid lesion to be considered as a designation of an "abnormal" hypermetabolic ^{18}F-FDG-avid focus and to be reported out as "suspicious for malignancy" was considered more complex than simply being based upon

Povoski *et al. BMC Cancer* (2015) 15:378

Page 3 of 8

its SUVmax, and also required the clinical judgment and expertise/experience of the reporting nuclear medicine physician.

Intraoperative gamma probe assessment was undertaken to all ^{18}F-FDG-avid tissue sites using various combinations of 6 different available gamma detection probe systems that were synchronously or dissynchronously available during the study period. Intraoperative gamma probe assessment of ^{18}F-FDG-avid tissue positivity was determined as based utilization of the concept of the three-sigma statistical threshold criteria. The three-sigma statistical threshold criteria for gamma probe positivity was previously popularized for radioimmuno-guided surgery by Thurston [70,75-77], and the derivation of its application to ^{18}F-FDG-avid tissue positivity was most recently articulated by Chapman et al. [75]. The three-sigma statistical threshold criteria was calculated by taking the standard deviation derived from the normal background tissue count rate and multiplying that standard deviation by a factor of three, and then adding that number to the normal background tissue count rate [70,75-77]. Using this statistical threshold methodology, intraoperative gamma probe assessment of ^{18}F-FDG-avid tissue positivity was confirmed when the count rate for the target tissue exceeded the three-sigma statistical threshold criteria [70,75]. A fixed ratiometric ^{18}F-FDG-avid lesion-to-background count ratio threshold was not utilized for the determination of probe positivity.

All continuous variables were expressed as mean value (± standard deviation; range). The software program IBM SPSS® 21 for Windows® (SPSS, Inc., Chicago, Illinois) was used for the data analysis. All mean value comparisons for continuous variables were performed by using the 2-tailed paired samples t-test. All categorical variable comparisons were made using 2 x 2 contingency tables that were analyzed by either the Pearson chi-square test or the Fisher exact test, when appropriate. P-values determined to be 0.05 or less were considered to be statistically significant.

Results

There were 13 patients with either suspected new lymphoma (n = 2) or suspected recurrent lymphoma (n = 11) that were available for the current analysis, as suggested by ^{18}F-FDG-avid lesions seen on their prior diagnostic whole-body PET/CT imaging. This included 10 females and 3 males. Their mean age was 51 (±16; range, 22–76) years. The mean SUVmax for the hottest ^{18}F-FDG-avid lesion seen on their most recent prior diagnostic whole-body PET/CT scans was 11.5 (±8.0; range, 1.7-25.6). The time of the most recent prior diagnostic whole-body PET/CT scan to the time of surgery was 13 (±17; range, 0–48) days.

The anatomical sites of the ^{18}F-FDG-avid lesions were 4 inguinal/groin region sites, 3 cervical region sites, 3 abdominal/retroperitoneal sites, 2 axillary region sites, and 1 gluteal subcutaneous tissue site. These anatomical sites of the ^{18}F-FDG-avid lesions were clinically palpable on physical examination in only 5 of the 13 patients.

These 13 patients were intravenously injected with ^{18}F-FDG prior to undergoing a same-day diagnostic lymph node surgical excisional biopsy procedure in the operating room, with a mean same-day ^{18}F-FDG injection dose of 14.8 (±2.4; range, 12.5-20.6) millicuries or 548 (±89; range, 463–762) megabecquerels (Table 1).

A same-day pre-resection patient PET/CT imaging was performed on 6 patients, including 4 same-day pre-resection whole body patient PET/CT scans and 2 same-day pre-resection limited field of view patient PET/CT scans. Intraoperative gamma probe assessment was performed on all 13 patients. Clinical scanner specimen PET/CT imaging of whole surgically excised tissue specimens was performed in 10 cases. Specimen gamma well counting was performed in 6 cases. A same-day post-resection limited field of view patient PET/CT imaging was performed on 8 patients.

As shown in Table 1, the time from ^{18}F-FDG injection to same-day pre-resection patient PET/CT was 76 (±8; range, 64–84) minutes. The time from ^{18}F-FDG injection to intraoperative gamma probe assessment was 240 (±63; range, 168–304) minutes. The time from ^{18}F-FDG injection to same-day post-resection limited field of view patient PET/CT was 487 (±104; range, 331–599) minutes. The time from ^{18}F-FDG injection to clinical scanner specimen PET/CT of whole surgically excised tissue specimens was 363 (±60; range, 272–446) minutes. The time from ^{18}F-FDG injection to specimen gamma well counting was 591 (±96; range, 420–689) minutes.

Intraoperative gamma probe assessment successfully identified the ^{18}F-FDG-avid lesion as probe positive (i.e., the ^{18}F-FDG-avid lesion/target tissue count rate exceeded the three-sigma statistical threshold criteria) in 12/13 patients that were probed. Clinical scanner specimen PET/CT imaging of whole surgically excised tissue specimens verified ^{18}F-FDG avidity within the sampled tissue from all 10 cases that were scanned. Same-day post-resection limited field of view patient PET/CT imaging verified successful removal of the intended ^{18}F-FDG-avid lesions in all 8 patients that were scanned.

Histopathologic evaluation confirmed lymphoma in 12/13 patients and benign disease (i.e., florid follicular hyperplasia) in 1/13 patients.

A representative example of a same-day pre-resection patient PET/CT scan and of a same-day post-resection patient PET/CT scan are shown in Figure 1 and of specimen PET/CT imaging of whole surgically excised tissue specimens is shown in Figure 2 for a specific case of histopathology-proven angioimmunoblastic T-cell lymphoma that originally presented as a non-palpable, ^{18}F-FDG

Povoski *et al. BMC Cancer* (2015) 15:378

Page 4 of 8

Table 1 Variables related to multimodal imaging and detection approach to ^{18}F-FDG-directed surgery

Variable	Mean value (± SD; range)
Same-day ^{18}F-FDG injection dose	14.8 (±2.4; 12.5-20.6) millicuries; or
	548 (±89; 463–762) megabecquerels
Time from ^{18}F-FDG injection to same-day pre-resection patient PET/CT	76 (±8; 64–84) minutes
Time from ^{18}F-FDG injection to intraoperative gamma probe assessment	240 (±63; 168–304) minutes
Time from ^{18}F-FDG injection to same-day post-resection limited field of view patient PET/CT	487 (±104; 331–599) minutes
Time from ^{18}F-FDG injection to clinical scanner specimen PET/CT of whole surgically excised tissue specimens	363 (±60; 272–446) minutes
Time from ^{18}F-FDG injection to specimen gamma well counting	591 (±96; 420–689) minutes

All variables are expressed as mean value (± standard deviation; range).
Abbreviations: ^{18}F-FDG ^{18}F-fluorodeoxyglucose, *PET/CT* positron emission tomography/computed tomography, *SD* standard deviation.

avid lesion within the right inguinal/groin region that was seen on a prior diagnostic patient PET/CT scan in a patient with a remote history of lymphoma.

Discussion

For lymphoma patients, it is well recognized that ^{18}F-FDG PET/CT imaging, in contrast to conventional anatomic imaging modalities (i.e., computed tomography, ultrasonography, or magnetic resonance imaging), allows for improved initial staging, treatment monitoring during therapy, restaging after completion of therapy, and detection of recurrent disease in the absence of any notably clinical and/or biochemical disease manifestations [1-13]. Along similar lines, ^{18}F-FDG PET/CT imaging allows for the recognition of a lesser degree of disease burden than is detectable on conventional anatomic imaging modalities, thus creating a situation in which patients with suspected new or suspected recurrent lymphoma will less frequently present with palpable adenopathy on clinical examination. Surgical biopsy continues to represent the principal diagnostic pathway by which a definitive tissue diagnosis is confirmed in patients with suspected new or suspected recurrent lymphoma [14]. With the improved detection of more limited disease burden by ^{18}F-FDG PET/CT
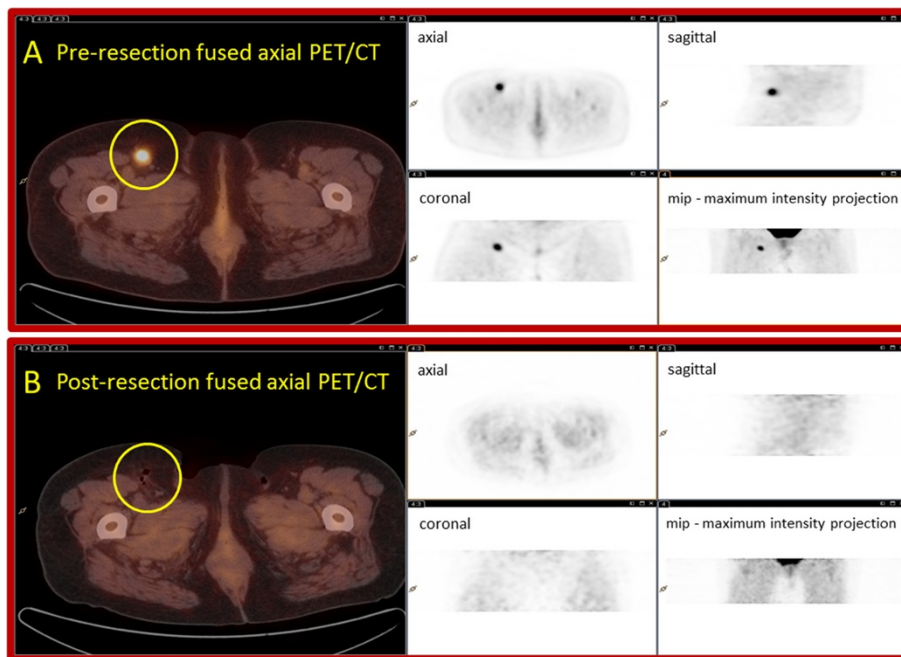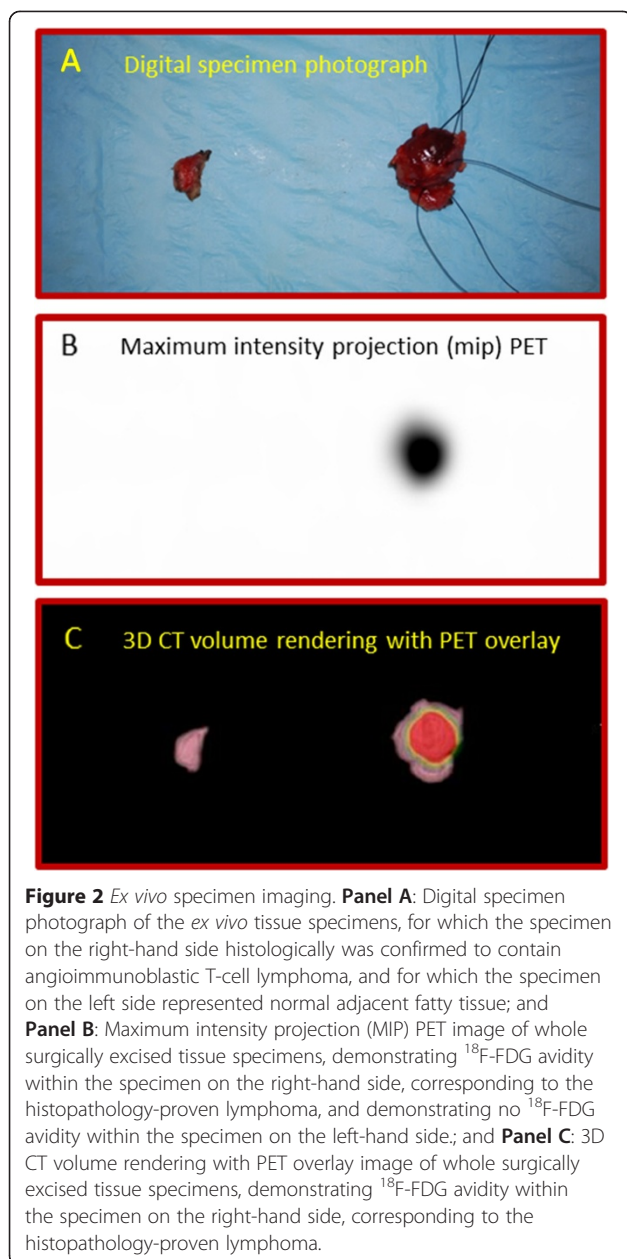

Figure 1 Patient imaging. Panel A: Same-day pre-resection whole body patient PET/CT scan images (i.e., fused PET/CT images and PET images) showing an isolated ^{18}F-FDG-avid lymph node (seen within the region of the yellow circle on the fused axial PET/CT image) in the right inguinal region which was not palpable on clinical examination; and **Panel B**: Same-day post-resection limited field of view patient PET/CT scan images (i.e., fused PET/CT images and PET images) showing successful removal of the intended ^{18}F-FDG-avid lymph node in the right inguinal region with residual air in the excision bed (seen within the region of the yellow circle on the fused axial PET/CT image).

Povoski *et al. BMC Cancer* (2015) 15:378

Page 5 of 8

Figure 2 *Ex vivo* specimen imaging. **Panel A**: Digital specimen photograph of the *ex vivo* tissue specimens, for which the specimen on the right-hand side histologically was confirmed to contain angioimmunoblastic T-cell lymphoma, and for which the specimen on the left side represented normal adjacent fatty tissue; and **Panel B**: Maximum intensity projection (MIP) PET image of whole surgically excised tissue specimens, demonstrating ^{18}F-FDG avidity within the specimen on the right-hand side, corresponding to the histopathology-proven lymphoma, and demonstrating no ^{18}F-FDG avidity within the specimen on the left-hand side.; and **Panel C**: 3D CT volume rendering with PET overlay image of whole surgically excised tissue specimens, demonstrating ^{18}F-FDG avidity within the specimen on the right-hand side, corresponding to the histopathology-proven lymphoma.

imaging, which is more frequently associated with an inability to appreciate palpable adenopathy on clinical examination, the surgeon's ability to successfully target the appropriate anatomical site of diagnostic tissue sampling for confirmation of the correct tissue diagnosis is made more challenging. Therefore, utilizing such innovative methodologies as a multimodal ^{18}F-FDG-directed lymph node surgical excisional biopsy approach for guiding appropriate diagnostic tissue sampling of lymph nodes detected as ^{18}F-FDG-avid lesions on diagnostic whole-body ^{18}F-FDG PET/CT imaging can help the surgeon to maximize the likelihood of success in establishing the correct tissue diagnosis. Likewise, such methodologies have

the potential for decreasing the degree of invasiveness as well as the degree of tissue disruption and tissue removal necessary for accomplishing successful tissue targeting.

Although we fully recognize that the current retrospective data analysis is based upon only 13 patients, the cases presented herein demonstrate that a multimodal ^{18}F-FDG-directed lymph node surgical excisional biopsy approach for suspected lymphoma is technically feasible for guiding appropriate diagnostic tissue sampling of lymph nodes seen as ^{18}F-FDG-avid lesions on diagnostic ^{18}F-FDG PET/CT imaging, especially when such ^{18}F-FDG-avid lesions are not easily appreciable as palpable adenopathy on clinical examination. Likewise, the conceptualization of this approach is well illustrated by the case presented in Figures 1 and 2. It is our belief that such a strategy can be best maximized when a multimodal imaging and detection approach is utilized involving perioperative patient and *ex vivo* surgical specimen ^{18}F-FDG PET/CT imaging in combination with intraoperative ^{18}F-FDG gamma probe detection. This line of reasoning has been validated by our group for a variety of disease-type-specific solid malignancies [16-18,33,35,36,38-41,43,44,46,47,52,61,69].

Along similar lines, three other groups of investigators have also previously described the successful utilization of commercially-available intraoperative hand-held gamma probe systems for ^{18}F-FDG-directed lymph node surgical excisional biopsy in patients with suspected or documented lymphoma [27,31,50,67]. Gulec et al. described this technique in four patients in one report from 2006 [27] and in six patients in another report from 2007 [31]. Molina et al. described this technique in three patients in their report from 2009 [50]. Vos et al. described this technique in one patient in their report from 2012 [67]. However, none of these three other groups of investigators utilized perioperative patient and *ex vivo* surgical specimen ^{18}F-FDG PET/CT imaging at the time of intraoperative ^{18}F-FDG gamma probe detection, thus falling short of incorporating a multimodal approach to this sometimes challenging diagnostic dilemma.

The ability to successfully perform an ^{18}F-FDG-directed lymph node surgical excisional biopsy procedure for suspected lymphoma is highly dependent upon the commercially-available intraoperative hand-held gamma probe that is used during such a surgical case. The most important performance parameters related to any given gamma detection probe system are generally thought to be: (1) overall sensitivity (i.e., efficiency); (2) spatial selectivity (i.e., radial sensitivity distribution); (3) spatial resolution (i.e., lateral sensitivity distribution); (4) energy resolution (i.e., spectral discrimination); and (5) contrast [46]. The most widely utilized commercially-available intraoperative hand-held gamma probes are generally designed for detecting radioisotopes of gamma-ray energies in the low-energy emission (0 keV to 150 keV) range

Povoski *et al. BMC Cancer* (2015) 15:378

Page 6 of 8

and medium-energy emission (150 keV to 400 keV) range, thus allowing successful detection of radioisotopes such as: (1) technetium-99 m (^{99m}Tc; 140 and 142 KeV; most commonly used for sentinel lymph node biopsy procedures and parathyroid surgery); (2) indium-111 (^{111}In; 171 and 247 KeV; used with octreotide to detect neuroendocrine tumors); (3) iodine-123 (^{123}I; 159 KeV; used with metaiodobenzylguanidine to detect neuroblastomas and pheochromocytomas); and (4) iodine-125 (^{125}I; 35 KeV; previously used with anti-TAG-72 monoclonal antibodies and anti-CEA monoclonal antibodies during radioimmunoguided surgery) [46,70].

However, most commercially-available intraoperative hand-held gamma probes are not specifically designed to directly or indirectly detect the resultant 511 KeV gamma emissions following positron annihilation emanating from higher energy gamma photon emitting/positron emitting radionuclides such as fluorine-18 (^{18}F) or iodine-124 (^{124}I) [46,70]. Resultantly, there has been a recent appearance of commercially-available intraoperative hand-held gamma probes that are specifically intended for attempting to detect 511 KeV gamma emissions from higher energy gamma photon emitting/positron emitting radionuclides. These commercially-available intraoperative hand-held gamma probes have generally been designated as "PET" probes. The overall weight and physical size of any typical "PET" probe is generally a function of the degree of physical side shielding/collimation necessary to theoretically block adjacent background radiation, to limit the field of view, and to collimate the head of the probe, with the intention of limiting the area of tissue contributing to the probe count rate and of providing better spatial resolution between areas of tissue of differing radioactivity levels [46,70,78]. Attempts at improving the current "PET" probe design by further increasing physical side shielding/collimation or by increasing crystal diameter/thickness to capture a higher percentage of 511 KeV gamma emissions would only result in a "PET" probe configuration prohibitively large in physical size, heavy in weight, and which would be much more costly [46,70,78], thus representing significant obstacles to applying the currently commercially-available "PET" probes to the detection of ^{18}F-FDG-avid tissues.

In order to attempt to bypass these physical barriers related to the degree of physical side shielding/collimation or crystal diameter/thickness in designing intraoperative hand-held gamma probes that are specifically intended for attempting to detect 511 KeV gamma emissions from higher energy gamma photon emitting/positron emitting radionuclides, engineering efforts have moved toward other directions for the adaptation of more novel "PET" probe designs that do not rely upon increasing physical side shielding/collimation or increasing crystal diameter/thickness. Examples of such alternative design concepts

that can be adapted to "PET" probe design are secondary K-alpha x-ray fluorescence [70,78], active electronic collimation [28,54,58,60,67,79-81], and other crystal geometry designs using multiple small crystals with specific novel geometric configurations [82,83] for optimizing background rejection capabilities. These innovative alternative design schemas for detecting higher energy gamma photon emitting/positron emitting radionuclides, some of which have already been successfully applied to intraoperative hand-held gamma probe designs, are also the focus of current pre-clinical research that is actively looking at developing small platform, portable perioperative and intraoperative patient and *ex vivo* surgical specimen imaging devices with similar capabilities for detecting higher energy gamma photon emitting/positron emitting radionuclides. However, such small platform, portable perioperative and intraoperative patient and *ex vivo* surgical specimen imaging devices have not yet been fully realized or made commercially available for use in the clinical arena.

Conclusions

A multimodal approach to ^{18}F-FDG-directed lymph node surgical excisional biopsy for suspected lymphoma is technically feasible for guiding appropriate diagnostic tissue sampling of lymph nodes seen as ^{18}F-FDG-avid lesions on prior diagnostic whole-body ^{18}F-FDG PET/CT imaging. This multimodal approach can be very helpful to the surgeon for accomplishing successful targeting of the appropriate anatomical sites (corresponding to ^{18}F-FDG-avid lesions) for successful diagnostic tissue sampling in confirming the correct tissue diagnosis in challenging cases involving patients with non-palpable suspected new or suspected recurrent lymphoma.

Povoski *et al. BMC Cancer* (2015) 15:378

Page 7 of 8

Author details
[1]Division of Surgical Oncology, Department of Surgery, Arthur G. James Cancer Hospital and Richard J. Solove Research Institute and Comprehensive Cancer Center, The Ohio State University Wexner Medical Center, Columbus, OH 43210, USA. [2]Division of Molecular Imaging and Nuclear Medicine, Department of Radiology, The Ohio State University Wexner Medical Center, Columbus, OH 43210, USA. [3]Division of Nuclear Medicine and Clinical Molecular Imaging, Department of Radiology, Hospital of the University of Pennsylvania, Philadelphia, PA 19104, USA.

References
1. Baba S, Abe K, Isoda T, Maruoka Y, Sasaki M, Honda H. Impact of FDG-PET/CT in the management of lymphoma. Ann Nucl Med. 2011;25:701–16.
2. Zanoni L, Cerci JJ, Fanti S. Use of PET/CT to evaluate response to therapy in lymphoma. Q J Nucl Med Mol Imaging. 2011;55:633–47.
3. Buchpiguel CA. Current status of PET/CT in the diagnosis and follow up of lymphomas. Rev Bras Hematol Hemoter. 2011;33:140–7.
4. Ansell SM, Armitage JO. Positron emission tomographic scans in lymphoma: convention and controversy. Mayo Clin Proc. 2012;87:571–80.
5. Alvarez Páez AM, Nogueiras Alonso JM, Serena Puig A. ^{18}F-FDG-PET/CT in lymphoma: two decades of experience. Rev Esp Med Nucl Imagen Mol. 2012;31:340–9.
6. Wu LM, Chen FY, Jiang XX, Gu HY, Yin Y, Xu JR. ^{18}F-FDG PET, combined FDG-PET/CT and MRI for evaluation of bone marrow infiltration in staging of lymphoma: a systematic review and meta-analysis. Eur J Radiol. 2012;81:303–11.
7. Manohar K, Mittal BR, Bhattacharya A, Malhotra P, Varma S. Fluoro-deoxy-glucose positron emission tomography/computed tomography in lymphoma: a pictorial essay. Indian J Nucl Med. 2013;28:85–92.
8. Kostakoglu L, Cheson BD. State-of-the-Art research on "lymphomas: role of molecular imaging for staging, prognostic evaluation, and treatment response". Front Oncol. 2013;3:212.
9. Allen-Auerbach M, de Vos S, Czernin J. PET/computed tomography and lymphoma. Radiol Clin North Am. 2013;51:833–44.
10. Kluge R, Kurch L, Montravers F, Mauz-Körholz C. FDG PET/CT in children and adolescents with lymphoma. Pediatr Radiol. 2013;43:406–17.
11. Nakayama M, Okizaki A, Ishitoya S, Sakaguchi M, Sato J, Aburano T. Dual-time-point F-18 FDG PET/CT imaging for differentiating the lymph nodes between malignant lymphoma and benign lesions. Ann Nucl Med. 2013;27:163–9.
12. Araf S, Montoto S. The use of interim (18)F-fluorodeoxyglucose PET to guide therapy in lymphoma. Future Oncol. 2013;9:807–15.
13. Barrington SF, Mikhaeel NG. When should FDG-PET be used in the modern management of lymphoma? Br J Haematol. 2014;164:315–28.
14. Morris-Stiff G, Cheang P, Key S, Verghese A, Havard TJ. Does the surgeon still have a role to play in the diagnosis and management of lymphomas? World J Surg Oncol. 2008;6:13.
15. Jaffe ES, Banks PM, Nathwani B, Said J, Swerdlow SH, Ad Hoc Committee on reporting of lymphoid neoplasms; Association of Directors of Anatomic and Surgical Pathology. Recommendations for the reporting of lymphoid neoplasms: a report from the Association of Directors of Anatomic and Surgical Pathology. Mod Pathol. 2004;17:131–5.
16. Desai D, Arnold M, Saha S, Hinkle G, Soble D, Frye J, et al. Intraoperative gamma detection of FDG distribution in colorectal cancer. Clin Positron Imaging. 1999;2:325.
17. Desai DC, Arnold M, Saha S, Hinkle G, Soble D, Fry J, et al. Correlative whole-body FDG-PET and intraoperative gamma detection of FDG distribution in colorectal cancer. Clin Positron Imaging. 2000;3:189–96.
18. Zervos EE, Desai DC, DePalatis LR, Soble D, Martin EW. ^{18}F-labeled fluorodeoxyglucose positron emission tomography-guided surgery for recurrent colorectal cancer: a feasibility study. J Surg Res. 2001;97:9–13.
19. Essner R, Hsueh EC, Haigh PI, Glass EC, Huynh Y, Daghighian F. Application of an [(18)F]fluorodeoxyglucose-sensitive probe for the intraoperative detection of malignancy. J Surg Res. 2001;96:120–6.
20. Essner R, Daghighian F, Giuliano AE. Advances in FDG PET probes in surgical oncology. Cancer J. 2002;8:100–8.
21. Higashi T, Saga T, Ishimori T, Mamede M, Ishizu K, Fujita T, et al. What is the most appropriate scan timing for intraoperative detection of malignancy using ^{18}F-FDG-sensitive gamma probe? Preliminary phantom and preoperative patient study. Ann Nucl Med. 2004;18:105–14.
22. Yap JT, Carney JP, Hall NC, Townsend DW. Image-guided cancer therapy using PET/CT. Cancer J. 2004;10:221–33.
23. Barranger E, Kerrou K, Petegnief Y, David-Montefiore E, Cortez A, Daraï E. Laparoscopic resection of occult metastasis using the combination of FDG-positron emission tomography/computed tomography image fusion with intraoperative probe guidance in a woman with recurrent ovarian cancer. Gynecol Oncol. 2005;96:241–4.
24. Carrera D, Fernandez A, Estrada J, Martin-Comin J, Gamez C. Detection of occult malignant melanoma by 18F-FDG PET-CT and gamma probe. Rev Esp Med Nucl. 2005;24:410–3 [Spanish].
25. Franc BL, Mari C, Johnson D, Leong SP. The role of a positron- and high-energy gamma photon probe in intraoperative localization of recurrent melanoma. Clin Nucl Med. 2005;30:787–91.
26. Kraeber-Bodéré F, Cariou B, Curtet C, Bridji B, Rousseau C, Dravet F, et al. Feasibility and benefit of fluorine 18-fluoro-2-deoxyglucose-guided surgery in the management of radioiodine-negative differentiated thyroid carcinoma metastases. Surgery. 2005;138:1176–82.
27. Gulec SA, Daghighian F, Essner R. PET-Probe. Evaluation of Technical Performance and Clinical Utility of a Handheld High-Energy Gamma Probe in Oncologic Surgery. Ann Surg Oncol. 2006; Jul 24; [Epub ahead of print].
28. Meller B, Sommer K, Gerl J, von Hof K, Surowiec A, Richter E, et al. High energy probe for detecting lymph node metastases with ^{18}F-FDG in patients with head and neck cancer. Nuklearmedizin. 2006;45:153–9.
29. Nwogu C, Fischer G, Tan D, Glinianski M, Lamonica D, Demmy T. Radioguided detection of lymph node metastasis in non-small cell lung cancer. Ann Thorac Surg. 2006;82:1815–20. discussion 1820.
30. Curtet C, Carlier T, Mirallié E, Bodet-Milin C, Rousseau C, Barbet J, et al. Prospective comparison of two gamma probes for intraoperative detection of ^{18}F-FDG: in vitro assessment and clinical evaluation in differentiated thyroid cancer patients with iodine-negative recurrence. Eur J Nucl Med Mol Imaging. 2007;34:1556–62.
31. Gulec SA, Hoenie E, Hostetter R, Schwartzentruber D. PET probe-guided surgery: applications and clinical protocol. World J Surg Oncol. 2007;5:65.
32. Gulec SA. PET probe-guided surgery. J Surg Oncol. 2007;96:353–7.
33. Hall NC, Povoski SP, Murrey DA, Knopp MV, Martin EW. Combined approach of perioperative ^{18}F-FDG PET/CT imaging and intraoperative ^{18}F-FDG handheld gamma probe detection for tumor localization and verification of complete tumor resection in breast cancer. World J Surg Oncol. 2007;5:143.
34. Piert M, Burian M, Meisetschlager G, Stein HJ, Ziegler S, Nahrig J, et al. Positron detection for the intraoperative localisation of cancer deposits. Eur J Nucl Med Mol Imaging. 2007;34:1534–44.
35. Sarikaya I, Povoski SP, Al-Saif OH, Kocak E, Bloomston M, Marsh S, et al. Combined use of preoperative ^{18}F FDG-PET imaging and intraoperative gamma probe detection for accurate assessment of tumor recurrence in patients with colorectal cancer. World J Surg Oncol. 2007;5:80.
36. Sun D, Bloomston M, Hinkle G, Al-Saif OH, Hall NC, Povoski SP, et al. Radioimmunoguided surgery (RIGS), PET/CT image-guided surgery, and fluorescence image-guided surgery: past, present, and future. J Surg Oncol. 2007;96:297–308.
37. Prior JO, Kosinski M, Delaloye AB, Denys A. Initial report of PET/CT-guided radiofrequency ablation of liver metastases. J Vasc Interv Radiol. 2007;18:801–3.
38. Agrawal A, Hall NC, Ringel MD, Povoski SP, Martin Jr EW. Combined use of perioperative TSH-stimulated ^{18}F-FDG PET/CT imaging and gamma probe radioguided surgery to localize and verify resection of iodine scan-negative recurrent thyroid carcinoma. Laryngoscope. 2008;118:2190–4.
39. Cohn DE, Hall NC, Povoski SP, Seamon LG, Farrar WB, Martin Jr EW. Novel perioperative imaging with ^{18}F-FDG PET/CT and intraoperative ^{18}F-FDG detection using a handheld gamma probe in recurrent ovarian cancer. Gynecol Oncol. 2008;110:152–7.
40. Hall NC, Povoski SP, Murrey DA, Knopp MV, Martin EW. Bringing advanced medical imaging into the operative arena could revolutionize the surgical care of cancer patients. Expert Rev Med Devices. 2008;5:663–7.

Povoski *et al. BMC Cancer* (2015) 15:378

Page 8 of 8

41. Moffatt-Bruce SD, Povoski SP, Sharif S, Hall NC, Ross Jr P, Johnson MA, et al. A novel approach to positron emission tomography in lung cancer. Ann Thorac Surg. 2008;86:1355–7.

42. Piert M, Carey J, Clinthorne N. Probe-guided localization of cancer deposits using [(18)F]fluorodeoxyglucose. Q J Nucl Med Mol Imaging. 2008;52:37–49.

43. Povoski SP, Hall NC, Martin EW, Walker MJ. Multimodality approach of perioperative ^{18}F-FDG PET/CT imaging, intraoperative ^{18}F-FDG handheld gamma probe detection, and intraoperative ultrasound for tumor localization and verification of resection of all sites of hypermetabolic activity in a case of occult recurrent metastatic melanoma. World J Surg Oncol. 2008;6:1.

44. Povoski SP, Sarikaya I, White WC, Marsh SG, Hall NC, Hinkle GH, et al. Comprehensive evaluation of occupational radiation exposure to intraoperative and perioperative personnel from ^{18}F-FDG radioguided surgical procedures. Eur J Nucl Med Mol Imaging. 2008;35:2026–34.

45. van Baardwijk A, Bosmans G, van Suylen RJ, van Kroonenburgh M, Hochstenbag M, Geskes G, et al. Correlation of intra-tumour heterogeneity on ^{18}F-FDG PET with pathologic features in non-small cell lung cancer: a feasibility study. Radiother Oncol. 2008;87:55–8.

46. Povoski SP, Neff RL, Mojzisik CM, O'Malley DM, Hinkle GH, Hall NC, et al. A comprehensive overview of radioguided surgery using gamma detection probe technology. World J Surg Oncol. 2009;7:11.

47. Murrey Jr DA, Bahnson EE, Hall NC, Povoski SP, Mojzisik CM, Young DC, et al. Perioperative (18)F-fluorodeoxyglucose-guided imaging using the becquerel as a quantitative measure for optimizing surgical resection in patients with advanced malignancy. Am J Surg. 2009;198:834–40.

48. Gollub MJ, Akhurst TJ, Williamson MJ, Shia J, Humm JL, Wong WD, et al. Feasibility of ex vivo FDG PET of the colon. Radiology. 2009;252:232–9.

49. Klaeser B, Mueller MD, Schmid RA, Guevara C, Krause T, Wiskirchen J. PET-CT-guided interventions in the management of FDG-positive lesions in patients suffering from solid malignancies: initial experiences. Eur Radiol. 2009;19:1780–5.

50. Molina MA, Goodwin WJ, Moffat FL, Serafini AN, Sfakianakis GN, Avisar E. Intra-operative use of PET probe for localization of FDG avid lesions. Cancer Imaging. 2009;9:59–62.

51. Mallarajapatna GJ, Kallur KG, Ramanna NK, Susheela SP, Ramachandra PG. PET/CT-guided percutaneous biopsy of isolated intramuscular metastases from postcricoid cancer. J Nucl Med Technol. 2009;37:220–2.

52. Hall NC, Povoski SP, Murrey DA, Martin Jr EW, Knopp MV. Ex vivo specimen FDG PET/CT imaging for oncology. Radiology. 2010;255:663–4.

53. Nalley C, Wiebeck K, Bartel TB, Bodenner D, Stack Jr BC. Intraoperative radiation exposure with the use of (18)F-FDG-guided thyroid cancer surgery. Otolaryngol Head Neck Surg. 2010;142:281–3.

54. de Jong JS, van Ginkel RJ, Slart RH, Lemstra CL, Paans AM, Mulder NH, et al. FDG-PET probe-guided surgery for recurrent retroperitoneal testicular tumor recurrences. Eur J Surg Oncol. 2010;36:1092–5.

55. Hartemink KJ, Muller S, Smulders YM, Petrousjka van den Tol M, Comans EF. Fluorodeoxyglucose F18(FDG)-probe guided biopsy. Ned Tijdschr Geneeskd. 2010;154:A1884 [Dutch].

56. Lee GO, Costouro NG, Groome T, Kashani-Sabet M, Leong SPL. The use of intraoperative PET probe to resect metastatic melanoma. BMJ Case Rep. 2010; doi:10.1136/bcr.12.2009.2593.

57. Klaeser B, Wiskirchen J, Wartenberg J, Weitzel T, Schmid RA, Mueller MD, et al. PET/CT-guided biopsies of metabolically active bone lesions: applications and clinical impact. Eur J Nucl Med Mol Imaging. 2010;37:2027–36.

58. García JR, Fraile M, Soler M, Bechini J, Ayuso JR, Lomeña F. PET/CT-guided salvage surgery protocol. Results with ROLL Technique and PET probe. Rev Esp Med Nucl. 2011;30:217–22 [Spanish].

59. Kim WW, Kim JS, Hur SM, Kim SH, Lee SK, Choi JH, et al. Radioguided surgery using an intraoperative PET probe for tumor localization and verification of complete resection in differentiated thyroid cancer: a pilot study. Surgery. 2011;149:416–24.

60. Manca G, Biggi E, Lorenzoni A, Boni G, Roncella M, Ghilli M, et al. Simultaneous detection of breast tumor resection margins and radioguided sentinel node biopsy using an intraoperative electronically collimated probe with variable energy window: a case report. Clin Nucl Med. 2011;36:e196–8.

61. Povoski SP, Hall NC, Murrey Jr DA, Chow AZ, Gaglani JR, Bahnson EE, et al. Multimodal imaging and detection approach to ^{18}F-FDG-directed surgery for patients with known or suspected malignancies: a comprehensive description of the specific methodology utilized in a single-institution cumulative retrospective experience. World J Surg Oncol. 2011;9:152.

62. Tatli S, Gerbaudo VH, Feeley CM, Shyn PB, Tuncali K, Silverman SG. PET/CT-guided percutaneous biopsy of abdominal masses: initial experience. J Vasc Interv Radiol. 2011;22:507–14.

63. Werner MK, Aschoff P, Reimold M, Pfannenberg C. FDG-PET/CT-guided biopsy of bone metastases sets a new course in patient management after extensive imaging and multiple futile biopsies. Br J Radiol. 2011;84:e65–7.

64. Sainani NI, Shyn PB, Tatli S, Morrison PR, Tuncali K, Silverman SG. PET/CT-guided radiofrequency and cryoablation: is tumor fluorine-18 fluorodeoxyglucose activity dissipated by thermal ablation? J Vasc Interv Radiol. 2011;22:354–60.

65. Francis CL, Nalley C, Fan C, Bodenner D, Stack Jr BC. ^{18}F-fluorodeoxyglucose and 131I Radioguided Surgical Management of Thyroid Cancer. Otolaryngol Head Neck Surg. 2012;146:26–32.

66. Bains S, Reimert M, Win AZ, Khan S, Aparici CM. A patient with psoriatic arthritis imaged with FDG-PET/CT demonstrated an unusual imaging pattern with muscle and fascia involvement: a case report. Nucl Med Mol Imaging. 2012;46:138–43.

67. Vos CG, Hartemink KJ, Muller S, Oosterhuis JW, Meijer S, van den Tol MP, et al. Clinical applications of FDG-probe guided surgery. Acta Chir Belg. 2012;112:414–8.

68. Hall N, Murrey D, Povoski S, Barker D, Zhang J, Bahnson E, et al. Evaluation of 18FDG PET/CT image quality with prolonged injection-to-scan times. Mol Imaging Biol. 2012;14(2, supplement):P610.

69. Hall NC, Povoski SP, Zhang J, Knopp MV, Martin Jr EW. Use of intraoperative nuclear medicine imaging technology: strategy for improved patient management. Expert Rev Med Devices. 2013;10:149–52.

70. Povoski SP, Chapman GJ, Murrey Jr DA, Lee R, Martin Jr EW, Hall NC. Intraoperative detection of ^{18}F-FDG-avid tissue sites using the increased probe counting efficiency of the K-alpha probe design and variance-based statistical analysis with the three-sigma criteria. BMC Cancer. 2013;13:98.

71. Cerci JJ, Pereira Neto CC, Krauzer C, Sakamoto DG, Vitola JV. The impact of coaxial core biopsy guided by FDG PET/CT in oncological patients. Eur J Nucl Med Mol Imaging. 2013;40:98–103.

72. Win AZ, Aparici CM. Real-time FDG PET/CT-guided bone biopsy in a patient with two primary malignancies. Eur J Nucl Med Mol Imaging. 2013;40:1787–8.

73. Cerci JJ, Huber FZT, Bogoni M. PET/CT-guided biopsy of liver lesions. Clin Transl Imaging. 2014;2:157–63.

74. Povoski SP, Murrey Jr DA, Smith SM, Martin Jr EW, Hall NC. ^{18}F-FDG PET/CT oncologic imaging at extended injection-to-scan acquisition time intervals derived from a single-institution ^{18}F-FDG-directed surgery experience: feasibility and quantification of ^{18}F-FDG accumulation within ^{18}F-FDG-avid lesions and background tissues. BMC Cancer. 2014;14:453.

75. Chapman GJ, Povoski SP, Hall NC, Murrey Jr DA, Lee R, Martin Jr EW. Comparison of two threshold detection criteria methodologies for determination of probe positivity for intraoperative in situ identification of presumed abnormal ^{18}F-FDG-avid tissue sites during radioguided oncologic surgery. BMC Cancer. 2014;14:667.

76. Thurston MO. Development of the gamma-detecting probe for radioimmunoguided surgery. In: Martin EW, editor. Radioimmunoguided Surgery (RIGS) in the Detection and Treatment of Colorectal Cancer, 1st edition. Austin: R.G. Landes Company; 1994. p. 41–65.

77. Martin Jr EW, Thurston MO. The use of monoclonal antibodies (MAbs) and the development of an intraoperative hand-held probe for cancer detection. Cancer Invest. 1996;14:560–71.

78. Martin EW, Chapman GJ, Subramaniam VV, Povoski SP. Intraoperative detection of gamma emissions using K-alpha X-ray fluorescence. Expert Rev Med Devices. 2010;7:431–4.

79. GFE Gesellschaft für Forschungs und Entwicklungsservice mbH); Gamma Locator DXI: [http://www.gfe-service.de/en/ylocator.php].

80. Gerl J, Ameil F, Kojouharov Z, , Surowiec D. High energy gamma probe with position sensing capability. European Patent EP 1 596 223 B1; Filed May 10, 2005; Published January 21, 2009.

81. Gerl J. Kojouharov Z, Ameil E, Surowiec D. High energy gamma probe with position sensing capability. United States Patent US 7,312,460 B2; Filed May 10, 2005; Published December 25, 2007.

82. Lecomte R, Schmitt D, Lamoureux G. Geometry study of a high resolution PET detection system using small detectors. IEEE T Nucl Sci. 1984;31:556–61.

83. Levin CS. New imaging technologies to enhance the molecular sensitivity of positron emission tomography. Proc IEEE. 2008;96:439–67.